NAVIGATED BRONCHOSCOPY USING INTRAOPERATIVE FLUOROSCOPY AND PREOPERATIVE CT

Teena Steger, Martin Hoßbach

Fraunhofer Institute for Computer Graphics Research IGD
Darmstadt, Germany

ABSTRACT

Bronchoscopic biopsies for diagnosis of lung cancer are usually done with the help of intraoperative fluoroscopy. But fluoroscopy images lack 3D information and do not provide a clear view of the bronchi or lesions.

Our goal is to enhance the physician's view by overlaying the intraoperative fluoroscopy images with both 2D and 3D airway visualizations from preoperatively taken CT scans. The presented system provides automatic airway segmentation and skeletonization as well as automatic 2D/3D alignment of fluoroscopy to CT. The results are used for correctly overlaying the airways and visualizing bronchoscopic paths. The only additional equipment needed is a specifically designed pattern of steel spheres and sticks on acrylic glass, which is fixed on the patient table. It is used for estimating the C-arm pose during image acquisition and allows 2D/3D image alignment in clinically feasible time ($<$6 s) and accuracy (mTRE$<$0.33 mm on simulated data). No interference with the physician's standard bronchoscopy procedure is introduced and no additional radiation exposure is required. On the contrary, by improving the physician's view and orientation inside the bronchial tree, a faster and more target-oriented guidance to the site of interest is possible.

***Index Terms*—** bronchoscopy, airway segmentation, c-arm pose estimation, 2D/3D, path calculation

1. INTRODUCTION AND RELATED WORK

Lung cancer is one of the most common cancer diagnoses with very little chances of cure. Biopsies from lung lesions are essential for diagnosis at an early stage, and therefore the success of the therapy. Bronchoscopy is the prevailing examination method for this. In addition to the camera of the bronchoscope, C-arms are widely used during the intervention for navigation. Fluoroscopy images display the position of the bronchoscope inside the airways. The physician uses this information to navigate the bronchoscope through the bronchial tree to the site of interest, e.g. suspicious tissue or lesions.

Unfortunately, a clear picture of the airways as well as a 3D visualization of the bronchial structures are missing on the fluoroscopy images. This impedes correct localization of the bronchoscope inside the branches and makes navigation difficult.

Several commercial guidance systems for bronchoscopic interventions are currently available on the market, among them the superDimension system[1] and the VIDA Diagnostics system[2]. Furthermore, researchers around the world explore intraoperative navigation for bronchoscopy. Except for some groups, who use the bronchoscopic video images for registration [1, 2], most of these systems attach electromagnetic trackers to the tip of the bronchoscope or the biopsy instrument [3, 4, 5]. Thus, the position of the instrument can be tracked during operation and marked inside a virtual visualization of the bronchial tree. But, using electromagnetic trackers normally means considerable additional effort and expenses for the physician or clinic, as the trackers need to be autoclavable or be costly replaced after each use. We believe it is preferable to maintain the established process the physician is used to and only optimize this process.

The standard process will be considerably improved, by fusing the rather poor presentation of the airways in the generally used fluoroscopy image with a well-visible 2D bronchial tree and a realistic 3D visualization of the same. This approach is also pursued by Xu *et al.*[6]. For obtaining the C-arm pose, which is needed for alignment of fluoroscopy to CT, they use feature-based 2D/3D registration. In contrast to them, we propose a method to calculate the C-arm pose *directly*, using computer vision methods performed on a specifically designed marker pattern. Thus, we achieve clinically feasible registration times and improved average accuracy in comparison to Xu *et al.* Also, we do not need manual initializations close to the optimum. Especially for real-time interventions like bronchoscopy, these aspects are of particular importance.

Our objective is to provide a clear and accurately positioned visualization (2D *and* 3D) of the bronchial tree, and also to locate the bronchoscope tip and path inside a 3D model of the tree. We assume, this will improve the physician's ability and speed to reach the destination as these system features considerably facilitate navigation.

[1] http://www.superdimension.com
[2] http://www.vidadiagnostics.com

2. MATERIALS AND METHODS

The proposed system for navigated bronchoscopy comprises three main components:

1. *Bronchial tree segmentation:* extract the bronchial tree from the preoperative CT volume
2. *C-arm pose estimation:* align the resulting 3D bronchial tree to the intraoperative fluoroscopy images
3. *Path calculation inside bronchial tree:* deduce the path of the bronchoscope using the skeletonization of the bronchial tree

Segmentation and skeletonization are done offline before the intervention. Pose estimation and path calculation need to be executed during the intervention in real-time. Subsequently, the bronchial tree and the path can be overlayed accurately both in 2D and 3D (see Fig. 2(a) and 2(c)). The following sections describe the individual components in more detail.

2.1. Bronchial tree segmentation

The state of the art in airway segmentation from CT data was summarized in the EXACT'09 workshop [7] at MICCAI 2009. Comparing the precision of the approaches as well as the complexity, we decided that the method suggested by Wiemker *et al.* was a very good compromise for our project. It provides reasonable results needing not too much time to complete. If a better segmentation is needed, it can be easily replaced. The following description is only a sketch of the algorithm; details and an evaluation of the algorithm can be found in [8]. A comparison of this algorithm with other approaches can be found in [7].

The approach of Wiemker *et al.* is based on (leakage-prone) region growing, extended by an algorithm calculating both centricity and radius for a certain voxel. We place a unit sphere at one voxel, uniformly sample the surface of this sphere, and then cast rays from the voxel through all points on the sphere's surface until they either hit a region of high density or the ray's length exceeds a certain threshold. The lengths of all rays not exceeding the length threshold, allow us to calculate the radius of the airway and a centricity measure. The latter can be regarded as the likelihood of the voxel being part of the airway centerline.

Using the voxel density, the centricity measure and the radius, a region growing is performed, such that voxel density needs to be below a certain threshold, centricity needs to be higher than a certain threshold, and the radius should decrease as the region growing moves down the trachea into the bronchi.

2.2. C-arm pose estimation

To obtain accurate alignment of preoperative CT to intraoperative fluoroscopy, the position and orientation of the C-arm to the *table* is sufficient, as very little movement by the sedated patient is expected. We use a marker pattern for this purpose (see Fig. 1(a)). It has an actual size of $100\,\mathrm{cm} \times 51\,\mathrm{cm}$ and consists of steel spheres with 3 mm diameter and steel sticks of 1.6 mm thickness and up to 12 mm length. Spheres and sticks are all arranged in one plane. If the pattern is placed on the patient table (as shown in Fig. 1(b)) or possibly embedded in it, they are well visible even on a fluoroscopy image (see Fig. 1(c)). Thus, 2D coordinates of projected image points in the fluoroscopy image and 3D coordinates of the pattern spheres on the patient table are available. Intrinsic camera parameters of the C-arm need to be calculated only once. Extrinsic parameters (respectively the pose) can be calculated during the intervention, after unambiguously mapping image to world coordinates.

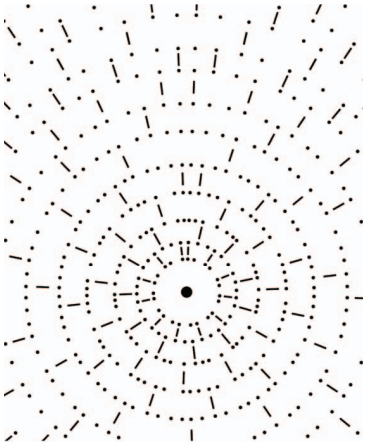
All parameters are determined using camera calibration methods, where known 3D world points $\mathbf{X} = [X, Y, Z]^T$ are projected using the projection matrix $\mathrm{P} = \mathrm{K}\left[\ \mathrm{R}\ \middle|\ \mathbf{t}\ \right]$, where R is the rotation matrix and $\mathbf{t}$ is the translation vector. Matrix K contains the intrinsic camera parameters. The sum of squares of error distances between the calculated 2D projection points $\mathbf{x}_p = \mathrm{P}\mathbf{X}_p = (u_p, v_p)^T$ and the detected 2D image points $\mathbf{x}_i = (u_i, v_i)^T$ is then minimized using iterative optimization to find the exact pose parameters.

It is essential that the coordinates of the image points $\mathbf{x}_i$ in the fluoroscopy image can always be mapped unambiguously to world coordinates of the source points $\mathbf{X}_p$ on the pattern. For assuring unambiguous mapping, the presented method uses collinear points, concurrent lines and the projective invariant: *cross-ratio*. Cross-ratio denotes a relation between point or angle distances. Its value remains the same, even after central projection of the points, respectively angles. It is defined as follows for points (*left*) and angles (*right*):

$$(ABCD) := \frac{(ABC)}{(ABD)} := \frac{\frac{\overline{AC}}{\overline{BC}}}{\frac{\overline{AD}}{\overline{BD}}} \quad (abcd) := \frac{\frac{\sin(\sphericalangle ac)}{\sin(\sphericalangle bc)}}{\frac{\sin(\sphericalangle ad)}{\sin(\sphericalangle bd)}} \qquad (1)$$

Thus, given four points or four angles, it is possible to calculate a cross-ratio value, which does not change even after central projection of the points or angles. Accordingly, comparing the cross-ratio of four source points in world coordinates to the cross-ratio of four image points in image coordinates is sufficient for unambiguously mapping them to each other, presupposed four collinear source points have a distinguishable cross-ratio value with regard to all other collinear source points. The same holds for angles likewise. The design of the pattern (see Fig. 1(a)) complies with these requirements.

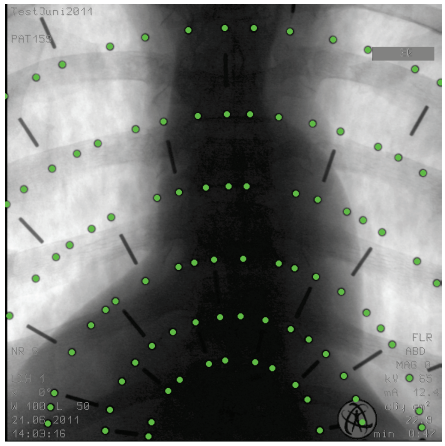
During the mapping process, circles (projected spheres) and lines (projected sticks) are segmented by performing a shape analysis of the connected components obtained from the Canny edge detector. Then, these lines are mapped to the corresponding source angles in the pattern using cross-



(a) Detail of the pattern design



(b) C-arm with marker pattern and thorax phantom on patient table



(c) Fluoroscopy of pattern and thorax phantom with reprojected points after pose estimation (green)

Fig. 1. Marker pattern for C-arm pose estimation

ratio values. Now, the circles are mapped line-by-line to the corresponding source points using cross-ratio again.

2.3. Path calculation inside bronchial tree

To calculate a path from the trachea to the tip of the bronchoscope, we use the results from both previous steps. First, the segmentation of the bronchial tree is skeletonized using the method by Drechsler *et al.* [9]. This method thins the airway to its centerline with a thickness of exactly one voxel. The root voxel is selected by iterating through the axial slices of the labelled volume. The first single voxel is used as the root.

The tip of the bronchoscope is manually selected on the fluoroscopy image by the physician. For calculating the location of the bronchoscope's tip inside the bronchi, the skeleton voxel associated to the selected pixel needs to be found. This is done by projecting all skeleton voxels into the fluoroscopy image using the previously estimated C-arm pose, which enables us to calculate a ray from the X-ray source through the thorax CT volume to any pixel in the fluoroscopy image (see Fig. 2(b)). Note that in case of superposed bronchi along the ray this will lead to multiple voxels in different branches as result. The projected skeleton voxels, whose distances to the selected pixel lie within a certain threshold, are chosen as candidates and then grouped by the skeleton branches they belong to. For each candidate branch the skeleton voxel with the smallest distance is selected as representative. These representatives are again sorted by distance and returned as a list where the first voxel is also the most probable spatial location of the bronchoscope's tip.

To find the path from the tip voxel to the root voxel, we relabel the skeleton using a depth first search. Starting at the root voxel with the label 1, the skeleton neighbours of the root voxel will be labelled with 2, their neighbours with 3, and so on. Now, we can find the path from any skeleton voxel (with label n) back to the root voxel, simply by iteratively looking for a voxel with label $n-1$ in the 8-neighbourhood.

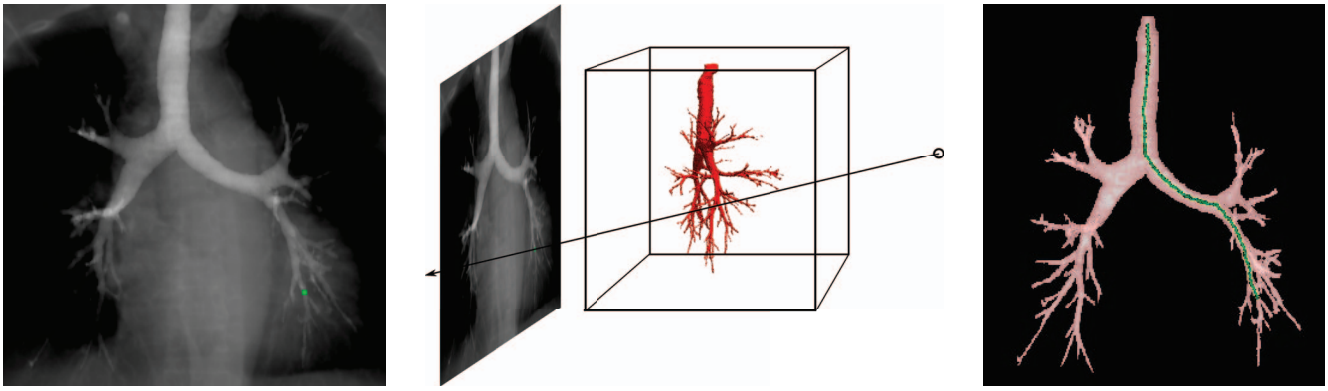
3. EVALUATION AND RESULTS

3.1. C-arm pose estimation

Evaluation with over 300 simulated DRRs of the pattern showed that the method achieves mean error values of 0.33 mm (3D) and 0.48 px (2D) for translations inside an imaging area of $30\,\mathrm{cm} \times 50\,\mathrm{cm}$ around the center of the pattern and rotations up to 30°. First tests on about 30 C-arm images (2 with thorax phantom) resulted in mean 2D accuracy values of 0.1–0.23 px. Fig. 1(c) exemplarily shows the result for a thorax phantom image. For this image, which is also the most challenging, execution time was less than 6 s (Intel Core i7 2.93 GHz). Hence, our pose estimation method is suitable for intraoperational use.

3.2. Path calculation inside bronchial tree

Path calculation was evaluated using segmentation and skeleton of a representative bronchial tree. 1500 voxels of the tree (1 %) were randomly selected and mapped to the nearest skeleton voxel in the same branch (target). Next, they were projected from 9 different rotational directions up to 30°. The projected pixels served as input to our path calculation algorithm. The resulting skeleton voxel list was then compared to the target. A test case was declared successful, if one of the resulting voxels belonged to the same path as the target. 97.8 % of all test cases were successful and in these cases the mean distance to the target voxel was 3.0 mm. This shows that the method is both robust and accurate. On average 5.7 voxels (in different paths) were returned as result. The voxel



(a) 2D overlay (DRR) of segmented airways with selected bronchoscope tip pixel (green)

(b) Ray from X-ray source through CT volume, bronchial tree segmentation/skeletonization (red) and selected pixel (green)

(c) 3D visualization of segmented airways with calculated bronchoscope path (green)

Fig. 2. 2D and 3D view of accurately located airway structures and bronchoscope path

with the smallest distance is recommended by the system and in 84.3 % this recommendation proved right. That means, in most cases the physician can rely on the system's recommendation. In some cases the physician will need to manually select additional image points of the bronchoscope or at worst acquire a new image from another position to exclude wrong branches. Execution time was less than 1 s for each selected pixel, which qualifies the method for intraoperational use.

4. CONCLUSIONS AND FUTURE WORK

We presented a new system for improved instrument guiding during bronchoscopy. The system provides automatic segmentation of the bronchial tree from CT data using a well-evaluated and robust algorithm with sufficient accuracy for our use case. Accurate and fast intraoperative alignment of fluoroscopy images to the CT volume is achieved by a novel and proprietary approach for C-arm pose estimation with a specially designed marker pattern. This method was evaluated on simulated data as well as on real C-arm images and a thorax phantom. For visualizing the bronchoscope path inside the bronchial tree, we developed a simple algorithm using skeletonization. Evaluation on simulated data promises robustness and high accuracy.

Our system adds plenty of information obtained from preoperative CT to the intraoperative scenario in clinically feasible time and accuracy. Thus, navigating through the airways to the site of interest is considerably facilitated.

Future work includes automatic bronchoscope detection, which will improve handling of ambiguities during path calculation, and further evaluation, especially on clinical data.

5. REFERENCES

[1] L. Rai et al., "Combined video tracking and image-video registration for continuous bronchoscopic guidance," *IJCARS*, vol. 3, pp. 315–329, Sept 2008.

[2] K. Mori et al., "Bronchoscope Tracking Based on Image Registration Using Multiple Initial Starting Points Estimated by Motion Prediction," in *MICCAI 2006*, 2006, pp. 645–652.

[3] I. Gergel et al., "In vitro Evaluation einer neuartigen elektromagnetischen Aspirationsnadel," in *Bildverarbeitung für die Medizin 2011*, Informatik aktuell, pp. 229–233. Springer Berlin Heidelberg, 2011.

[4] T. D. Soper et al., "In vivo validation of a hybrid tracking system for navigation of an ultrathin bronchoscope within peripheral airways," *IEEE Trans Biomed Eng*, vol. 57, pp. 736–745, Mar 2010.

[5] Y. Schwarz et al., "Real-time electromagnetic navigation bronchoscopy to peripheral lung lesions using overlaid CT images: the first human study," *Chest*, vol. 129, pp. 988–994, Apr 2006.

[6] D. Xu et al., "Single-view 2D/3D registation for x-ray guided bronchoscopy," in *Proc. of the 2010 IEEE ISBI*, Piscataway, NJ, USA, 2010, ISBI'10, pp. 233–236, IEEE Press.

[7] P. Lo et al., "Extraction of airways from ct (exact'09)," in *2nd Intl. Wksp. on Pulm. Imag. Anal.*, 2009, pp. 175–189.

[8] R. Wiemker et al., "A simple centricity-based region growing algorithm for the extraction of airways," in *2nd Intl. Wksp. on Pulm. Imag. Anal.*, 2009, pp. 309–314.

[9] K. Drechsler et al., "Hierarchical decomposition of vessel skeletons for graph creation and feature extraction," in *Proc. of IEEE Intl. Conf. BIBM*, 2010, pp. 456 –461.